

# Cosmological and astrophysical aspects of finite-density QCD

D. J. Schwarz<sup>a</sup> \*

<sup>a</sup>Institut für Theoretische Physik, Universität Frankfurt,  
Postfach 11 19 32, 60054 Frankfurt am Main, Germany

The different phases of QCD at finite temperature and density lead to interesting effects in cosmology and astrophysics. In this work I review some aspects of the cosmological QCD transition and of astrophysics at high baryon density.

## 1. Introduction

In the early universe, at high temperatures and almost vanishing chemical potential, we expect from asymptotic freedom that quarks and gluons are deconfined in a quark-gluon plasma (QGP). As the universe cools by expansion, a transition to the confined phase, a hadron gas (HG), occurs at  $T_* \sim \Lambda_{\text{QCD}}$ . Lattice QCD at vanishing chemical potential provides important insight into the nature of the cosmological QCD transition [1].

In the most compact stars, neutron stars or quark stars, another transition associated with QCD might happen. The dense phase might be a QGP at high chemical potential and low temperature, or it might be color superconducting phase [2,3] of diquarks. Between the cosmological and the astrophysical branch of the QCD phase diagram is the region where heavy ion collisions [4] take place.

In Sec. 2 I sketch the evolution of the baryon density and the baryon chemical potential during the expansion of the universe. The baryon chemical potential is almost zero in the very early universe. After the annihilation of all anti-baryons (at  $T_{\text{ann}} \sim m_p/25$ ) the baryon chemical potential is approximately equal to the nucleon rest mass.

The cosmological QCD transition is discussed in Sec. 3. I show that strangelet formation [5] and inhomogeneous nucleosynthesis [6] are unlikely consequences of the QCD transition. The reason is the small mean bubble separation (much smaller than the Hubble radius) [7,8], which follows from recent lattice QCD results for latent heat and surface tension [9]. At scales larger than the bubble separation the sound speed vanishes during the transition [10,11]. This means that density perturbations fall freely during the transition giving rise to large amplifications of the primordial density spectrum at small scales [10]. This leads to the formation of small clumps of cold dark matter ( $M_{\text{clump}} < 10^{-10} M_{\odot}$ ), for cold dark matter which is kinetically decoupled at the QCD scale, e.g. axions. The large drop in relativistic degrees of freedom during the QCD transition modifies the spectrum of primordial gravitational waves [12].

High baryon densities are realized in compact astrophysical bodies like neutron, hybrid, or (strange) quark stars. Lattice QCD cannot deal with a finite chemical potential so far

---

\*e-mail: dschwarz@th.physik.uni-frankfurt.de

[13], therefore the equation of state of dense matter is unknown. Toy models, like the bag model are used instead. Observable consequences of the high density phase(s) might be visible in the cooling curves of neutron stars [14,15]. A phase transition inside a pulsar might be observed as severe spin-up of the pulsar, as recently shown by Glendenning, Pei, and Weber [16].

Finally, I comment on the ultimate heavy 'ion' collision, the collision of two neutron stars. It has been suggested that such an event might be the central engine of short gamma-ray bursts [17].

## 2. Baryon number density and chemical potential

At high temperatures ( $T > \Lambda_{\text{QCD}}$ ) the baryon number density may be defined as  $n_{\text{B}} \equiv \frac{1}{3} \sum (n_q - n_{\bar{q}})$ , where  $n_q$  ( $n_{\bar{q}}$ ) is the number density of a specific quark (anti-quark) flavor, and the sum is taken over all quark flavors. At  $T < 1$  GeV only the u, d, and s quarks contribute significantly. At low temperatures ( $T < \Lambda_{\text{QCD}}$ ) the baryon number density is defined as  $n_{\text{B}} \equiv \sum (n_b - n_{\bar{b}})$ , now the summation is taken over all baryon species. Practically the nucleons contribute to the baryon number of the universe only.

Below the electroweak transition ( $T_{\text{ew}} \sim 300$  GeV) the baryon number,  $B$ , in a comoving volume is conserved. On the other hand entropy,  $S$ , is conserved. As a consequence the ratio of baryon number density and entropy density,  $s$ , is constant. From the abundances of primordial  ${}^4\text{He}$  and D [produced in big bang nucleosynthesis (BBN)] we know the ratio  $n_{\text{B}}/n_{\gamma} = (1.5 \text{ to } 6.3) \times 10^{-10}$  [18]. Taking into account the three massless neutrinos along with the photons that contribute to the entropy density, we find

$$\frac{n_{\text{B}}}{s} = (2 \text{ to } 8) \times 10^{-11} . \quad (1)$$

Due to this very small ratio the number of quarks equals the number of anti-quarks in the very early universe.

Let me now turn to the baryon chemical potential. At high temperatures the quark chemical potentials,  $\mu_q$ , are equal, because weak interactions keep them in chemical equilibrium (e.g.  $u + e \leftrightarrow d$  or  $s + \nu_e$ ), and the chemical potentials for the leptons are assumed to vanish (see [19] for a discussion of lepton chemical potentials). Thus, the chemical potential for a baryon is defined by  $\mu_{\text{B}} \equiv 3\mu_q$ . For an anti-baryon the chemical potential is  $-\mu_{\text{B}}$ . The baryon number density of an ideal Fermi gas of three quark flavors reads  $n_{\text{B}} \approx T^2 \mu_{\text{B}}/3$  at high temperature  $T$ . From Eq. (1) we find that

$$\frac{\mu_{\text{B}}}{T} \sim 10^{-9} \quad \text{at } T > \Lambda_{\text{QCD}} . \quad (2)$$

Thus, lattice QCD at finite temperature and vanishing chemical potential is most appropriate to study the QCD equation of state for the early universe.

At low temperatures ( $T < \Lambda_{\text{QCD}}$ )  $\mu_{\text{B}} = \mu_{\text{p}} = \mu_{\text{n}}$ , neglecting the mass difference between the proton and the neutron. The ratio of baryon number density and entropy now reads

$$\frac{n_{\text{B}}}{s} \approx 0.05 \left( \frac{m_{\text{p}}}{T} \right)^{\frac{3}{2}} \exp \left( -\frac{m_{\text{p}}}{T} \right) \sinh \left( \frac{\mu_{\text{B}}}{T} \right) . \quad (3)$$

Since this ratio is constant, the behavior of  $\mu_B/T$  is given by Eq. (3), e.g. at  $m_p/T \approx 20$  we find  $\mu_B/T \approx 10^{-2}$ . All anti-baryons are annihilated when the ratio

$$\frac{n_b - n_{\bar{b}}}{n_b + n_{\bar{b}}} \approx \tanh\left(\frac{\mu_B}{T}\right) \quad (4)$$

goes to unity. This happens when  $\mu_B/T \sim 1$ , which corresponds to  $m_p/T_{\text{ann}} \approx 25$  or  $T_{\text{ann}} \approx 40$  MeV. Below this temperature the baryon chemical potential is  $\mu_B(T \ll T_{\text{ann}}) \approx m_p$ . To add one proton to the universe one proton rest mass should be invested.

### 3. The cosmological QCD transition

Recent lattice QCD results for two quark flavors suggest that QCD makes a transition at a temperature of  $T_* \sim 150$  MeV [1,20]. Lattice calculations with three quark flavors indicate that the transition is of first order for the physical mass of the strange quark [21]. These calculations use Wilson quarks. However, with staggered quarks it has been concluded that the QCD transition is a crossover for the physical quark masses [22]. I therefore discuss a first order QCD transition and a QCD crossover below.

Lattice QCD with quenched quarks shows a first order transition with a latent heat  $l = 1.4T_*^4$  and a surface tension  $\sigma = 0.015T_*^3$  [9]. These values are much smaller than the values suggested by the bag model.  $l$  and  $\sigma$  are not known for the physical masses of the quarks (there is just an upper limit  $\sigma < 0.1T_*^3$  [23]).

The scale of the cosmological QCD transition is given by the Hubble radius,  $R_H$ , at the transition, which is  $R_H \sim m_{\text{Pl}}/T_*^2 \sim 10$  km. The mass inside the Hubble volume is  $\sim 1M_\odot$ . The expansion time scale is  $10^{-5}$  s, which should be compared with the time scale of QCD,  $1 \text{ fm}/c \approx 10^{-23}$  s. All interaction rates are much higher than the expansion rate of the universe. Even the rate of weak interactions,  $\Gamma_w \sim G_F^2 T^5$ , exceeds the Hubble rate,  $H \sim T^2/m_{\text{Pl}}$ , by a factor  $10^7$ . Therefore photons, leptons, quarks and gluons (or pions) are tightly coupled and may be described as a single, adiabatically expanding fluid.

The cosmological QCD transition causes a dramatic drop in the number of relativistic degrees of freedom,  $g_*$ . In the quark-gluon plasma  $g_*^{\text{QGP}} = 61.75(51.25)$  with(out) the strange quark, whereas for the hadron gas  $g_*^{\text{HG}} = 17.25(21.25)$  including pions (plus kaons and eta) besides the photon and leptons ( $e, \mu, \nu$ s).

This large drop in degrees of freedom modifies the spectrum of primordial gravitational waves [12]. One source of primordial gravitational waves is inflation [24]. These gravitational waves are produced with an almost scale invariant spectrum, i.e. the root mean square (rms) amplitude  $h_f$  of frequency  $f$  is the same for all frequencies at horizon crossing,  $f = H$ . After horizon crossing the energy density of the gravitational waves is redshifted, i.e.  $\rho_{\text{gw}} \sim m_{\text{Pl}}^2 f^2 h_f^2 \sim a^{-4}$ , where  $a$  is the scale factor of the universe. Without the QCD transition this results in a constant energy density of gravitational waves per frequency interval,  $\Omega_{\text{gw}}(f) \equiv (d\rho_{\text{gw}}/d \ln f)/\rho_{\text{crit}} = \text{const.}$ , for modes that cross the Hubble radius before radiation-matter equality. If we now take the large drop of degrees of freedom during the QCD transition into account, the Hubble radius evolves as  $R_H \sim g_*^{1/6}(a)a^2$ . On the other hand, physical scales grow like  $a$ . Thus, the number of modes that enter the Hubble radius per time interval changes, and therefore the slope of  $\Omega_{\text{gw}}(f)$  changes during the QCD transition. Modes that enter after the transition are unaffected, whereas

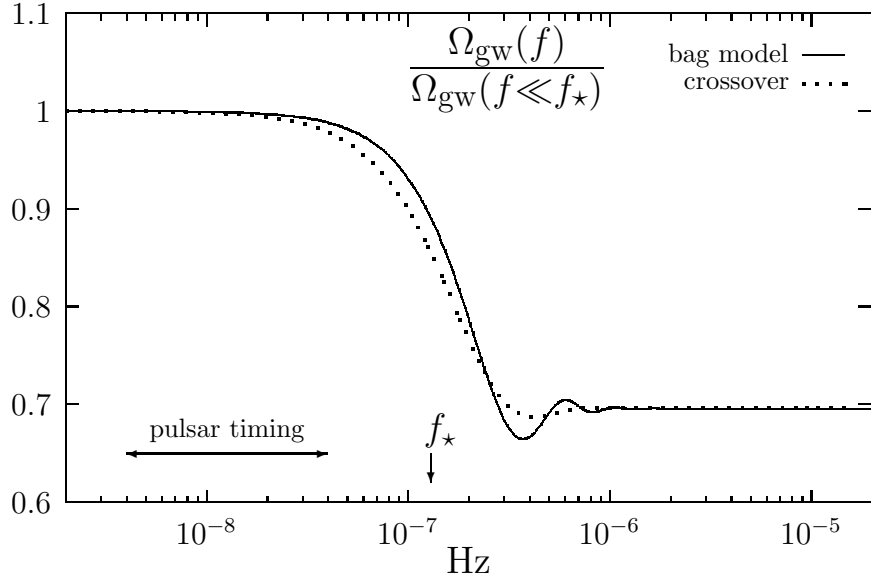


Figure 1. The modification of the energy spectrum, per logarithmic frequency interval, for primordial gravitational waves from the QCD transition [12].

modes that enter long before the transition are suppressed by a factor

$$\frac{\Omega_{\text{gw}}(f \gg f_*)}{\Omega_{\text{gw}}(f \ll f_*)} = \left( \frac{g_*^{\text{HG}}}{g_*^{\text{QGP}}} \right)^{\frac{1}{3}} \approx 0.7 . \quad (5)$$

This step is shown in Fig. 1. It is also demonstrated that this step in the spectrum is the same for a first order phase transition (bag equation of state) and for a crossover (interpolation between both phases by a tanh). The chances to detect this step in pulsar timing residuals [25] in the near future is poor, because the expected rms amplitude of primordial gravitational waves is orders of magnitudes below the current pulsar timing sensitivity. However, the only observable consequence of a QCD crossover is, to my knowledge, the step in the spectrum of gravitational waves.

### 3.1. Effects from the bubble separation scale

For a first order QCD transition hadronic bubbles nucleate during a short period of supercooling,  $\Delta t_{\text{sc}} \sim 10^{-8}$  s [7]. The typical bubble nucleation distance is a few cm for homogeneous nucleation [8], which is  $d_{\text{nuc1}} \approx 10^{-6} R_{\text{H}}$ . The hadronic bubbles grow very fast, until the released latent heat has reheated the universe to  $T_*$ . This happens almost instantaneously. The increase in entropy due to this reheating is just  $\Delta S \sim 10^{-6} S$ . For the remaining 99.9% of the transition the HG and the QGP coexist at the pressure

$$p_* \equiv p_{\text{HG}}(T_*) = p_{\text{QGP}}(T_*) . \quad (6)$$

During this time the hadronic bubbles grow slowly and the release of latent heat keeps the temperature constant until the transition is completed. At the end of the transition only few quark droplets are left over, with a typical separation  $d_{\text{nuc1}}$ .

In the mid 80s interest in the cosmological QCD transition arose, because it was realized that a strong first order QCD phase transition could lead to important observable signatures. Witten [5] pointed out that a separation of phases during the coexistence of the hadronic and the quark phase could gather most baryons in (strange) quark nuggets [26,5]. These would contribute to the dark matter today. At the end of the transition the baryon number in the quark droplets could exceed the baryon number in the hadron phase by several orders of magnitude,  $n_B^{\text{QGP}}$  could be close to nuclear density [27]. However, it was realized that the quark nuggets, while cooling, lose baryons. The quark nuggets evaporate, unless they contain much more than  $10^{44}$  baryons initially [28]. This number should be compared with the number of baryons inside a Hubble volume at the QCD transition, which is  $10^{50}$ . Thus, the mean bubble nucleation distance should be  $> 10^{-2}R_H \sim 100$  m in order to collect enough baryons.

In [27,28] a chromoelectric flux tube model was used to estimate the penetration rate of baryons through the interface. A quark that tries to penetrate the interface creates a flux tube, which most probably breaks up into a quark anti-quark pair. By this mechanism mesons evaporate easily. On the other hand baryons are formed rarely, because a diquark anti-diquark pair has to be produced in the break up of the flux tube. One could easily think of mechanisms that would increase the evaporation rate of baryons [29]. If a significant fraction of diquarks was formed in the quark phase, these diquarks could penetrate the interface by creating a flux tube, which eventually breaks creating a quark anti-quark pair. The quark would leave together with the diquark and form a baryon, whereas the anti-diquark would remain in the quark phase. Such a mechanism would increase the evaporation rate dramatically. In this case even unrealistically large values of  $d_{\text{nucl}}$  would not give rise to the formation of strangelets.

Applegate and Hogan found that a strong first order QCD phase transition induces inhomogeneous nucleosynthesis [18]. It is extremely important to understand the initial conditions for BBN, because many of our ideas about the early universe rely on the validity of the standard (homogeneous) BBN scenario. The standard BBN scenario is in good agreement with observations [18]. In inhomogeneous nucleosynthesis large isothermal fluctuations of the baryon number (the remnants of the quark droplets at the end of the QCD transition) could lead to different yields of light elements. As a minimal requirement for an inhomogeneous scenario of nucleosynthesis the mean bubble nucleation distance has to be larger than the proton diffusion length, which corresponds to  $\sim 3$  m [30] at the QCD transition. This is two orders of magnitude above recent estimates of the typical nucleation distance [8]. On the other hand the observed cosmic abundances of light elements do not favor inhomogeneous nucleosynthesis, except a small region in parameter space corresponding to an inhomogeneity scale of  $\sim 40$  m [30].

The above effects deal with physics at the bubble separation scale. It was assumed that the mean bubble separation is large ( $\sim 100$  m), because latent heat and surface tension had been overestimated in the past. Recent lattice QCD calculations [9] find smaller values for latent heat and surface tension and therefore the mean bubble nucleation distance is just a few cm.

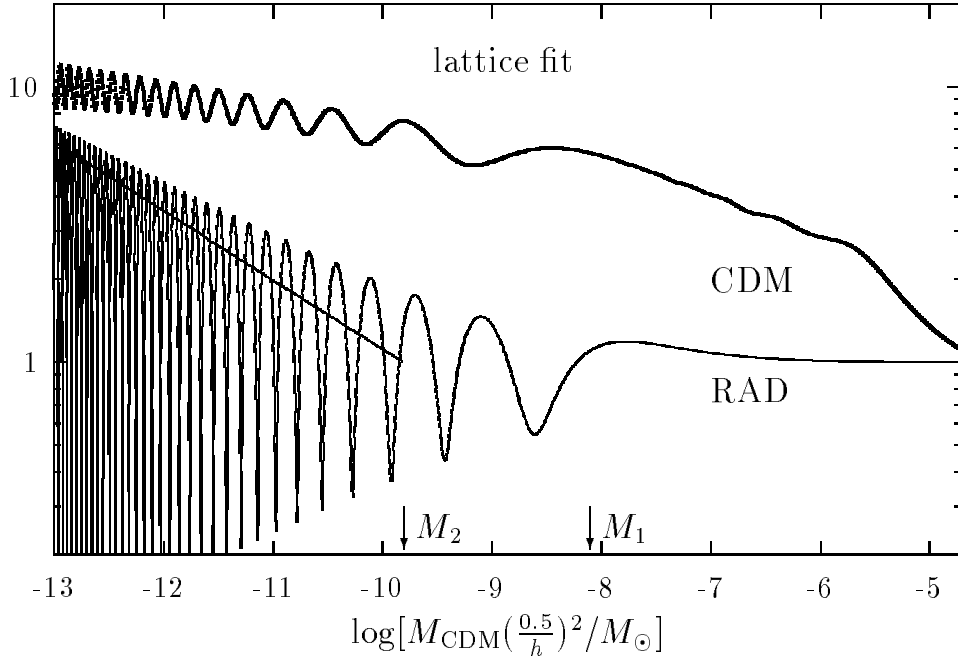


Figure 2. The modifications of the density contrast,  $\delta \equiv \delta\rho/\rho$ , of kinetically decoupled CDM (like axions) and of the radiation fluid fluctuation amplitude (RAD) due to the QCD transition as obtained in [10]. Both quantities are normalized to the pure Harrison-Zel'dovich radiation amplitude. On the horizontal axis the wavenumber  $k$  is represented by the CDM mass contained in a sphere of radius  $\pi/k$ . The QCD equation of state has been fitted to lattice QCD results [32,33]. The straight line starts at  $M_2$  and shows the asymptotic envelope for small scales  $\propto k^{3/4}$ . The CDM mass inside the Hubble radius is denoted  $M_1$ .

### 3.2. Effects from the Hubble scale

Scales  $\lambda$  that are of the order of the Hubble radius  $R_H$  are not sensitive to details of the bubbles. Together with Schmid and Widerin I found in Ref. [10] that the evolution of cosmological density perturbations is strongly affected by a first order QCD transition for subhorizon scales,  $\lambda < R_H$ . Cosmological perturbations on all scales are predicted by inflation [31] and have been observed in the temperature fluctuations of the cosmic microwave background by the COBE satellite [34].

In the radiation dominated universe subhorizon density perturbations perform acoustic oscillations. The restoring force is provided by pressure gradients. The pressure gradients, hence the isentropic sound speed  $c_s = (\partial p / \partial \rho)_s^{1/2}$  (on scales much larger than the bubble separation scale) drops to zero at a first order QCD transition [10], because both phases coexist at the pressure  $p_*$  only ( $a$  is the scale factor of the universe):

$$c_s^2 \equiv \left( \frac{\partial p}{\partial \rho} \right)_s = \frac{dp_*/da}{d\rho(a)/da} = 0. \quad (7)$$

It stays zero during the entire transition and suddenly rises back to the radiation value  $c_s = 1/\sqrt{3}$  after the transition. A significant decrease in the effective sound speed  $c_s$

during the cosmological QCD transition was pointed out by Jedamzik [11] independently. Pressure varies continuously and goes below the ideal radiation fluid value  $p = \rho/3$ , but stays positive.

As the sound speed drops to zero, the restoring force for acoustic oscillations vanishes and density perturbations for subhorizon modes fall freely. The fluid velocity stays constant during this free fall. Perturbations of shorter wavelengths have higher velocities at the beginning of the transition, and thus grow proportional to wavenumber  $k$  during the phase transition. The primordial Harrison-Zel'dovich spectrum of density perturbations is amplified on subhorizon scales. It develops peaks which grow, at most, linearly in wavenumber, see Fig. 2. We used a fit to the QCD equation of state obtained on the lattice [32,33]. The spectrum of density perturbations on superhorizon scales,  $\lambda > R_H$ , is unaffected. At  $T \sim 1$  MeV the neutrinos decouple from the radiation fluid. During this decoupling the large peaks in the radiation spectrum are wiped out by collisional damping.

Today the universe is dominated by dark matter, most likely cold dark matter (CDM). If CDM is kinetically decoupled from the radiation fluid at the QCD transition, the density perturbations in CDM do not suffer from the neutrino damping. This is the case for primordial black holes or axions, but not for supersymmetric dark matter. At the time of the QCD transition the energy density of CDM is small, i.e.  $\rho^{\text{CDM}}(T_*) \sim 10^{-8} \rho^{\text{RAD}}(T_*)$ . CDM falls into the potential wells provided by the dominant radiation fluid. Thus, the CDM spectrum is amplified on subhorizon scales, see Fig. 2. The peaks in the CDM spectrum go nonlinear shortly after radiation-matter equality. This leads to the formation of CDM clumps with mass  $< 10^{-10} M_\odot$ . Especially the clumping of axions has important implications for axion searches with strong magnetic fields [35]. If the QCD transition is strong enough, there is a chance that these clumps could be detected by gravitational femtolensing [36].

The vanishing of the sound speed during the coexistence phase also leads to interesting gravitational effects, as pointed out by Jedamzik [11]. He found that the probability to form black holes is enhanced during the QCD transition due to the vanishing pressure gradients. These black holes have masses  $\sim 1 M_\odot$ . He claims that black holes from the QCD transition could account for the massive compact halo objects (MACHO's) observed by microlensing [37] in the halo of our galaxy. However, for standard models of structure formation (standard CDM,  $\Lambda$ CDM, etc.) the amplitude of fluctuations at the QCD horizon crossing scale is not big enough to produce a cosmologically relevant amount of black holes. A fine tuned primordial spectrum would be necessary.

#### 4. Neutron stars — quark stars

In this section I concentrate on observable aspects of compact stars. A neutron star mostly consists of neutrons, but due to weak interactions it has an admixture of protons and electrons ( $\mu_n = \mu_p + \mu_e$ ). The equation of state is a function of two chemical potentials (if we neglect temperature), because there are two conserved charges, baryon number and electric charge. If the chemical potentials are high enough, heavier particles contribute to the star's composition ( $\mu$ ,  $\pi$ ,  $\Lambda$ , etc.). Besides the hadron core (with energy densities  $\rho \sim 10^{15}$  g/cm<sup>3</sup>  $\sim \Lambda_{\text{QCD}}^4$ ) the star has a crust of iron (with  $\rho < 10^{13}$  g/cm<sup>3</sup>). An extensive

discussion of the structure and properties of compact stars can be found in [38].

Asymptotic freedom of QCD suggests that at high baryon chemical potential a deconfinement transition happens. The core of the neutron star may consist of a phase of free quarks and gluons [39]. An extended mixed phase might exist, because charge has to be conserved globally, but not locally [40]. Such objects are called hybrid stars. If strange matter (made of u, d, and s quarks) is absolutely stable the star is called quark star (or strange star). The details of the hybrid and quark stars' composition and structure strongly depend on the equations of state of QCD and nuclear matter [16,41].

An important feature of neutron stars is their strong magnetic field (typically  $10^7$  T). When a neutron star rotates fast enough, the magnetic dipole radiates. The neutron star can be observed as pulsar (more than 730 have been detected). Some pulsars stand alone and some come in binaries. For the binary systems the mass of the pulsar can be obtained (about 20 masses are known). The mean mass is  $\sim 1.4M_\odot$  [42], the maximum mass is  $\sim 1.8M_\odot$  (Vela X-1). The pulsar ages are known if the supernova from which the pulsar formed has been observed (Crab) and/or some remnants from the supernova explosion are observable. Another way to estimate the pulsar age starts from the assumption that the spin-down is due to the magnetic dipole only. In this case  $\tau_{\text{dipole}} \equiv \dot{P}/(2P)$ , where  $P$  is the period of the pulsar. Surface temperatures of pulsars have been measured for a couple of pulsars by the X-ray satellites ROSAT and ASCA [43]. Fig. 3 shows the surface temperature and dipole age for four pulsars.

Can observations decide which is the correct model for neutron stars? Of course, every model should include masses as large as the heaviest observed pulsar. Another prediction from the models is the cooling curve. After a supernova explosion the remaining central star is hot and has to cool by emitting neutrinos mainly. The cooling rate crucially depends on the kind of allowed weak (so-called Urca) processes, like  $p + e \rightarrow n + \nu_e$  (direct Urca). If the fraction of protons is small, the triangle inequality between the Fermi momenta,  $p_F^e + p_F^p \geq p_F^n$ , is violated and the direct Urca processes are forbidden. In this case only modified Urca processes and/or neutrino bremsstrahlung can occur and cooling is slower. For neutron stars with a core of nucleons below some critical proton fraction, the slow cooling scenario applies. Higher densities or more exotic matter (hyperons, kaon condensate, etc.) enhance the cooling [45,14]. The same happens for a quark core [46]. A recent calculation for competing models [strange star (SM) and neutron star (NS), both with enhanced (1) and standard cooling (2)] has been performed by Schaab et al. [15], see Fig. 3. A comparison with observations seems to slightly prefer the suppression of direct Urca processes (models SM-2 and NS-2 fit better than model SM-1 and NS-1 in Fig. 3). Another set of calculations includes superfluid phases in neutron stars and strange stars. These models do not show significant differences in their cooling behavior.

These findings might support the ideas of Alford, Rajagopal, and Wilczek [2], who argue that a color-flavor locked state might exist in the core of a quark star. Due to the locking of flavor, the direct Urca processes should be suppressed (similar to the superfluid models of [15]). The color-flavor locked phase exists, if there is some attractive force between two quarks (there is an attractive one-gluon-exchange diagram, but the next order is repulsive; a non-perturbative answer is needed). Other observational consequences of the color-flavor locked state remain to be investigated [3].

Pulsar timing is one of the most precise experiments in nature. Not only the angular



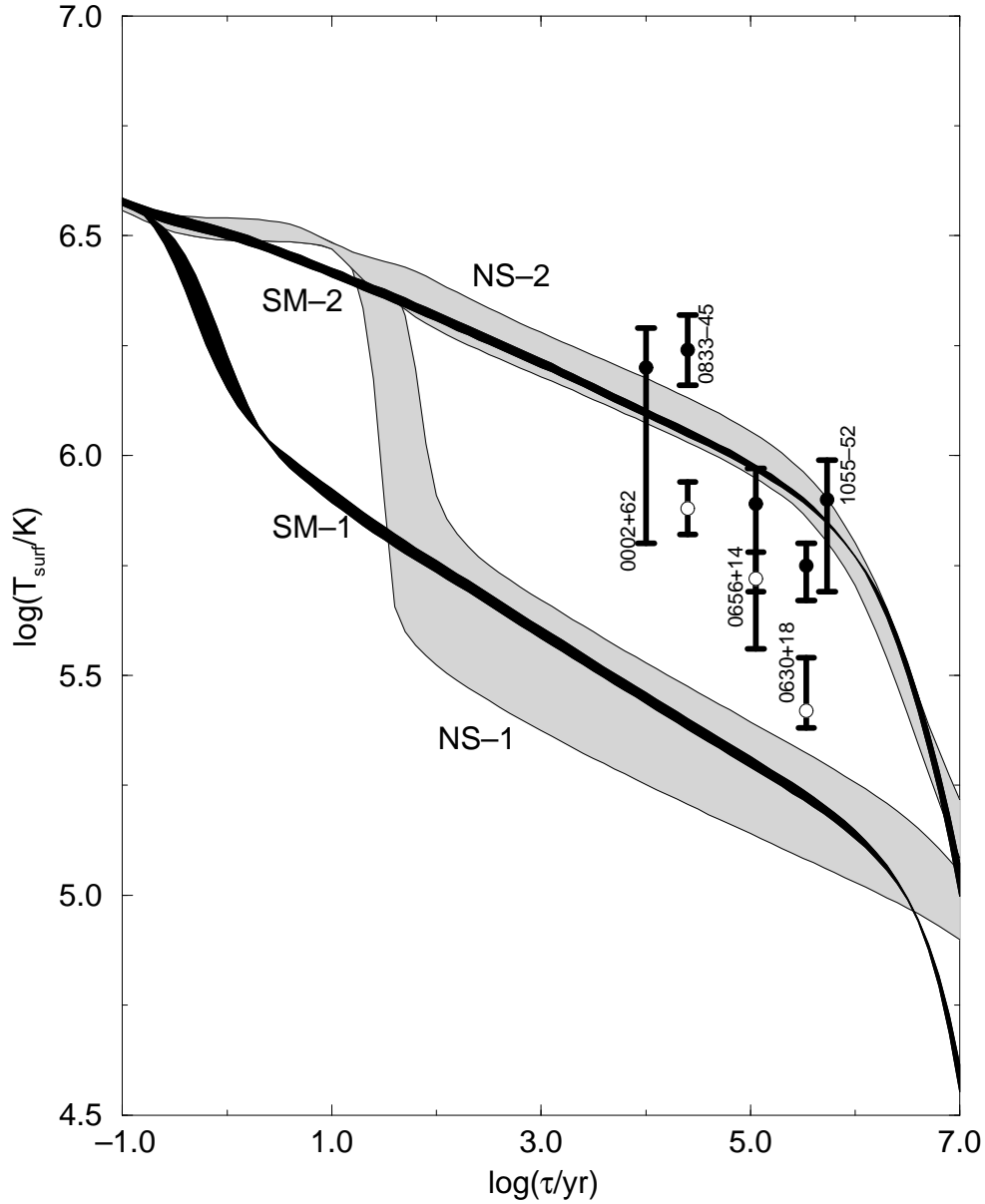


Figure 3. The cooling behavior of non-superfluid strange matter stars SM-1 (lower solid band) and SM-2 (upper solid band) and non-superfluid neutron stars NS-1 (lower shaded band) and NS-2 (upper shaded band). The surface temperatures of several observed neutron stars obtained for a blackbody (magnetic hydrogen) atmosphere are marked with error bars with solid (hollow) circles. Courtesy of F. Weber [44].

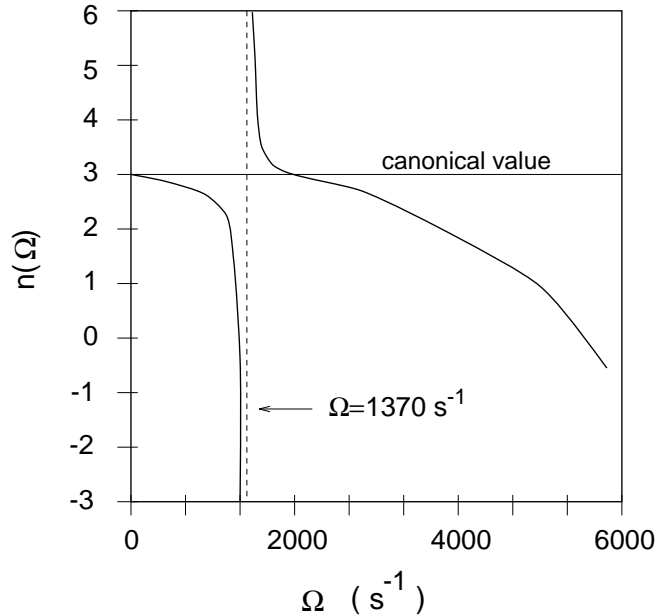


Figure 4. The braking index  $n$  as a function of rotational frequency for a hybrid star. The dip at frequencies  $\Omega \sim 1370 \text{ s}^{-1}$  originates from quark deconfinement. The overall reduction of  $n$  below 3 is due to the frequency dependence of the moment of inertia and, thus, is independent of whether or not quark deconfinement takes place in pulsars. Courtesy of F. Weber [44].

velocity of a pulsar can be measured, but also its first and second derivatives. This allows to look for phase transitions inside the pulsar. This important effect has been discovered recently by Glendenning, Pei, and Weber [16]. Pulsars are decelerated by electromagnetic emission and by a wind of electrons and positrons. As a pulsar slows down, its central density increases. At some critical density a phase transition might occur. The radius of the star shrinks, and the moment of inertia decreases. Since angular momentum is conserved, this causes a period of spin-up, which lasts about  $2 \times 10^7$  years (a 1/50th of the pulsar's spin-down time). The most interesting observable is the braking index  $n \equiv \ddot{\Omega}\Omega/\dot{\Omega}^2$  ( $\Omega$  is the angular velocity), which grows to large values  $|n| \gg 3$  (see Fig. 4). This would be a unique signature of a phase transition. The prospects to actually measure such spin-ups are reasonably good. About 1/50th of all pulsars might pass through such a phase currently. So far, the braking index has been measured for a few pulsars only.

Let me finally comment on the ultimate heavy 'ion' collision, a collision of two neutron stars. It has been suggested that collisions of neutron stars might be the source of short gamma-ray bursts [17]. A large number of gamma-ray bursts (GRB), the most energetic events in the universe, have been detected in the recent years by the BATSE instrument on the CGRO spacecraft [47]. Their distribution is isotropic across the sky and they are placed at cosmological distances, as demonstrated by the recent discoveries of X-ray, optical, and radio transients [48]. For the GRB of 14 December 1997 the host galaxy was identified at a redshift of  $z = 3.42$  [49]. This large distance implies that about  $3 \times 10^{53}$  erg, corresponding to a rest-mass energy of  $0.2M_{\odot}$ , have been released in  $\gamma$ -rays. Energy released in neutrinos or gravitational waves is not included in this number. The observed

durations of GRBs vary from several ms to  $10^3$  s. The observed photons have energies up to 26 GeV [50].

To understand the origin of GRBs several mechanisms have been proposed. The models have in common that the observed GRBs stem from a relativistic fireball (with Lorentz factor  $> 100$ ) [51]. The so-called central engine of the fireball is unknown. A promising scenario is the merging of two neutron stars [52]. All neutron star binaries lose energy by gravitational radiation, finally they spiral in and merge. Such events are expected to happen at a rate  $10^{-6}$  per year per galaxy, which allows to observe about one event per day.

A even more dramatic scenario has been suggested in Ref. [17]. The collision of two neutron stars in very dense clusters of stars could account for short (ms) GRBs. Numerical simulations of neutron star collisions have been performed in [53]. The authors find an extremely luminous outburst of neutrinos. From the annihilation of neutrinos and anti-neutrinos a fireball of electrons and positrons with the right amount of energy is formed. However, they find a large baryon contamination of the fireball, too large to explain the observed GRB. However, the dependence of this result on the equation of state has not been investigated. A soft point in the equation of state certainly would change the baryon contamination. As in the cosmological QCD transition a first order transition could give rise to small sound speed, and pressure gradients could be much smaller than in the simulations [53], giving rise to slower expansion of the baryon fluid.

## 5. Conclusions

The success of standard big bang nucleosynthesis suggests that the cosmological QCD transition is either a smooth crossover, or, in the case of a first order transition, latent heat  $l$  and surface tension  $\sigma$  are restricted by  $v^2\sigma^3/(l^2T_\star) < 100$ . This bound follows from  $d_{\text{nucl}} < d_{\text{proton diffusion}} \sim 10^{-4}R_{\text{H}}$ , using the analytical results for  $d_{\text{nucl}}$  of [7].  $v$  is the velocity at which the released latent heat is transported into the quark phase, a good guess might be  $v \sim 0.1c$ . This bound is consistent with lattice QCD results [9].

For a cosmological QCD transition of first order we expect clumps in CDM that is kinetically decoupled at the QCD scale (axions or primordial black holes) [10]. This would reduce the chances to detect axions in ongoing searches [35]. A further study of the evolution of clumped CDM is needed to give quantitative answers, a better knowledge of the QCD equation of state (from lattice QCD) is needed to predict the size of these clumps.

A QCD transition inside a neutron star could be detected by the severe spin-up of pulsars [16]. Pulsar timing needs long periods of observation, thus, patience is required.

Cooling curves of pulsars might be a tool to rule out some of the equations of state for matter at high baryon density. Progress in the calculation of equations of state at high baryon chemical potential on the lattice is of major importance for a better understanding of the most compact stars in the universe.

The collision of two neutron stars might give new insight into the equation of state in neutron stars. These collisions might have been observed in short gamma-ray bursts [17].

## Acknowledgment

I am grateful to M. Hofmann, M. Hanauske, J. Ignatius, F. Weber, and P. Widerin for discussions and/or comments on the manuscript. I thank the Alexander von Humboldt foundation for financial support.

## REFERENCES

1. For recent reviews see K. Kanaya, Nucl. Phys. B (Proc. Suppl.) **47**, 144 (1996); E. Laermann, Nucl. Phys. B (Proc. Suppl.) **63**, 141 (1998).
2. M. Alford, K. Rajagopal, and F. Wilczek, Phys. Lett. B **422**, 247 (1998); e-print hep-ph/9804403 (1998); R. Rapp et al., e-print hep-ph/9711396 (1997); J. Berges and K. Rajagopal, e-print hep-ph/9804233 (1998).
3. F. Wilczek, contributions to this volume.
4. N. Herrmann, contribution to this volume.
5. E. Witten, Phys. Rev. D **30**, 272 (1984).
6. J. H. Applegate and C. J. Hogan, Phys. Rev. D **31**, 3037 (1985); J. H. Applegate, C. J. Hogan, and R. J. Scherrer, Phys. Rev. D **35**, 1151 (1987); G. M. Fuller, G. J. Mathews, and C. R. Alcock, Phys. Rev. D **37**, 1380 (1988); R. A. Malaney and G. J. Mathews, Phys. Rep. **229**, 145 (1993).
7. J. Ignatius et al., Phys. Rev. D **49**, 3854 (1994); **50**, 3738 (1994).
8. M. B. Christiansen and J. Madsen, Phys. Rev. D **53**, 5446 (1996).
9. Y. Iwasaki et al., Phys. Rev. D **46**, 4657 (1992); **49**, 3540 (1994); B. Beinlich, F. Karsch, and A. Peikert, Phys. Lett. B **390**, 268 (1997).
10. C. Schmid, D. J. Schwarz, and P. Widerin, Phys. Rev. Lett. **78**, 5468 (1997).
11. K. Jedamzik, Phys. Rev. D **55**, 5871 (1997).
12. D. J. Schwarz, e-print gr-qc/9709027.
13. I. Barbour, contribution to this volume.
14. C. J. Pethick, Rev. Mod. Phys. **64**, 1133 (1992); C. Schaab et al., Nucl. Phys. **A605**, 531 (1996).
15. C. Schaab et al., Astrophys. J. **480**, L111 (1997).
16. N. K. Glendenning, S. Pei, and F. Weber, Phys. Rev. Lett. **79**, 1603 (1997).
17. J.I. Katz and L. M. Canel, Astrophys. J. **471**, 915 (1996); V. I. Dokuchaev and Yu. N. Eroshenko, Sov. Astron. Lett. **22**, 578 (1996).
18. For a recent review on big bang nucleosynthesis see C. Caso et al., Eur. Phys. J. **C3**, 1 (1998), available on the PDG WWW pages (URL:<http://pdg.lbl.gov/>).
19. S. Weinberg, *Gravitation and Cosmology* (John Wiley & Sons, New York, 1972).
20. C. Bernard et al., Phys. Rev. D **54**, 4585 (1996).
21. Y. Iwasaki et al., Z. Phys. C **71**, 343 (1996); Nucl. Phys. B (Proc. Suppl.) **47**, 515 (1996).
22. F. R. Brown et al., Phys. Rev. Lett. **20**, 2491 (1990).
23. M. Hackel et al., Phys. Rev. D **46**, 5648 (1992).
24. A. A. Starobinskii, Pis'ma Zh. Eksp. Teor. Fiz. **30**, 719 (1979) [JETP Lett. **30**, 682 (1979)].
25. V. M. Kaspi, J. H. Taylor, and M. F. Ryba, Astrophys. J. **428**, 713 (1994); S. E.

- Thorsett and R. J. Dewey, Phys. Rev. D **53**, 3468 (1996); M. P. McHugh et al., Phys. Rev. D **54**, 5993 (1996).
26. A. Bodmer, Phys. Rev. D **4**, 1601 (1971); E. Farhi and R. L. Jaffe, Phys. Rev. D **30**, 2379 (1984).
  27. K. Sumiyoshi et al., Phys. Rev. D **42**, 3963 (1990).
  28. K. Sumiyoshi and T. Kajino, Nucl. Phys. B (Proc. Suppl.) **24**, 80 (1991); P. Bhattacharjee et al., Phys. Rev. D **48**, 4630 (1993).
  29. This mechanism for enhanced baryon penetration through the phase interface was pointed out to me by M. Hofmann.
  30. In-Saeng Suh and G. J. Mathews, e-print astro-ph/9805179 (1998).
  31. V. Mukhanov and G. Chibisov, Pis'ma Zh. Eksp. Teor. Fiz. **33**, 549 (1981) [JETP Lett. **33**, 532 (1981)]; A. Starobinsky, Phys. Lett. B **117**, 175 (1982); A. Guth and S.-Y. Pi, Phys. Rev. Lett. **49**, 1110 (1982); S. Hawking, Phys. Lett. B **115**, 295 (1982).
  32. G. Boyd et al., Phys. Rev. Lett. **75**, 4169 (1995); Nucl. Phys. **B469**, 419 (1996).
  33. MILC Collaboration, Phys. Rev. D **55**, 6861 (1997).
  34. G. F. Smoot et al., Astrophys. J. **396**, L1 (1992).
  35. P. Sikivie, Phys. Rev. Lett. **51**, 1415 (1983); C. Hagmann et al., Phys. Rev. Lett. **80**, 2043 (1998).
  36. A. Gould, Astrophys. J. **386**, L5 (1992); A. Ulmer and J. Goodman, Astrophys. J. **442**, 67 (1995).
  37. MACHO Collaboration, Astrophys. J. **486**, 697 (1997); EROS Collaboration, Astron. Astrophys. **324**, L69 (1997).
  38. N. K. Glendenning, *Compact Stars* (Springer, New York, 1997).
  39. N. Itho, Prog. Theor. Phys. **44**, 291 (1970); G. Baym and S. Chin, Phys. Lett. **62B**, 241 (1976); G. Chaplin and M. Nauenberg, Nature **264**, 235 (1976); B. D. Keister and L. S. Kisslinger, Phys. Lett. **64B**, 117 (1976).
  40. N. K. Glendenning, Phys. Rev. D **46**, 1274 (1992).
  41. N. K. Glendenning and F. Weber, Astrophys. J. **400**, 647 (1992); C. Kettner et al., Phys. Rev. D **51**, 1440 (1995).
  42. S. E. Thorsett, et al., Astrophys. J. **405**, L29 (1992).
  43. C. Greiveldinger et al., Astrophys. J. **465**, L35 (1996) and references therein.
  44. F. Weber, *Pulsars as Astrophysical Laboratories for Nuclear and Particle Physics*, to be published by IOP Publishing Co, Bristol, England.
  45. J. Boguta, Phys. Lett. B **106**, 255 (1981); J. M. Lattimer et al., Phys. Rev. Lett. **66**, 2701 (1991).
  46. N. Iwamoto, Phys. Rev. Lett. **44**, 1637 (1980); Ann. Phys. (N.Y.) **141**, 1 (1982).
  47. C. A. Meegan et al., Astrophys. J. Suppl. Ser. **106**, 65 (1996).
  48. E. Costa et al., Nature **387**, 783 (1997); J. van Paradijs et al., Nature **386**, 686 (1997); D. A. Frail et al., Nature **389**, 261 (1997).
  49. S. R. Kulkarni et al., Nature **393**, 35 (1998).
  50. G. J. Fishman et al., Astron. Astrophys. Suppl. Ser. **97**, 17 (1993).
  51. For two recent reviews see P. Mészáros, e-print astro-ph/9711354 (1997); T. Piran, e-print astro-ph/9801001 (1998).
  52. Eichler et al., Nature **340**, 126 (1989).
  53. M. Ruffert and H. Th. Janka, e-print astro-ph/9804132 (1998).